

# *Staphylococcus aureus* and *Escherichia coli* dual-species biofilms on nanohydroxyapatite loaded with CHX or ZnO nanoparticles

Joana Barros,<sup>1,2,3\*</sup> Liliana Grenho,<sup>1,2,3\*</sup> Sílvia Fontenente,<sup>2,4,5</sup> Cândida M. Manuel,<sup>5,6</sup> Olga C. Nunes,<sup>5</sup> Luís F. Melo,<sup>5</sup> Fernando J. Monteiro,<sup>1,2,3</sup> Maria P. Ferraz<sup>7</sup>

<sup>1</sup>FEUP – Faculdade de Engenharia, Departamento de Engenharia Metalúrgica e Materiais, Universidade do Porto, Portugal

<sup>2</sup>i3S – Instituto de Investigação e Inovação em Saúde, Universidade do Porto, Portugal

<sup>3</sup>INEB – Instituto de Engenharia Biomédica, Universidade do Porto, Portugal

<sup>4</sup>IPATIMUP – Institute of Molecular Pathology and Immunology of the University of Porto, Portugal

<sup>5</sup>LEPABE – Laboratory for Process Engineering, Environment, Biotechnology and Energy, Departamento de Engenharia Química, Universidade do Porto, Portugal

<sup>6</sup>ULP–Universidade Lusófona do Porto, Portugal

<sup>7</sup>FP-ENAS/CEBIMED, University Fernando Pessoa Energy, Environment and Health Research Unit/Biomedical Research Center, Porto, Portugal

Received 11 August 2016; revised 14 September 2016; accepted 3 October 2016

Published online 31 October 2016 in Wiley Online Library (wileyonlinelibrary.com). DOI: 10.1002/jbm.a.35925

**Abstract:** Implant-associated infections are caused by surface-adhering microorganisms persisting as biofilms, resistant to host defense and antimicrobial agents. Given the limited efficacy of traditional antibiotics, novel strategies may rely on the prevention of such infections through the design of new biomaterials. In this work, two antimicrobial agents applied to nanohydroxyapatite materials—namely, chlorhexidine digluconate (CHX) and zinc oxide (ZnO) nanoparticles—were compared concerning their ability to avoid single- or dual-species biofilms of *Staphylococcus aureus* and *Escherichia coli*. The resulting biofilms were quantified by the enumeration of colony-forming units and examined by confocal microscopy using both Live/Dead staining and bacterial-specific fluorescent *in situ* hybridization. The sessile population arrangement was also observed by scanning electron microscopy. Both

biomaterials showed to be effective in impairing bacterial adhesion and proliferation for either single- or dual-species biofilms. Furthermore, a competitive interaction was observed for dual-species biofilms wherein *E. coli* exhibited higher proliferative capacity than *S. aureus*, an inverse behavior from the one observed in single-species biofilms. Therefore, either nanoHA-CHX or nanoHA-ZnO surfaces appear as promising alternatives to antibiotics for the prevention of device-related infections avoiding the critical risk of antibiotic-resistant strains emergence. © 2016 Wiley Periodicals, Inc. J Biomed Mater Res Part A: 105A: 491–497, 2017.

**Key Words:** nanohydroxyapatite, chlorhexidine digluconate, zinc oxide nanoparticles, single-species biofilm, dual-species biofilm, FISH

**How to cite this article:** Barros J, Grenho L, Fontenente S, Manuel CM, Nunes OC, Melo LF, Monteiro FJ, Ferraz MP. 2017. *Staphylococcus aureus* and *Escherichia coli* dual-species biofilms on nanohydroxyapatite loaded with CHX or ZnO nanoparticles. J Biomed Mater Res Part A 2017;105A:491–497.

## INTRODUCTION

Medical implants are highly susceptible to infection, either because of a locally acquired host defense defect or because implants offer a ready interface to which individual microorganisms may attach and rapidly form a biofilm.<sup>1,2</sup> The establishment of a biofilm thus includes initial microbial adhesion to a surface, followed by multiplication, resulting in microcolonies of single or multispecies of microorganisms (bacteria and/or fungi). Further maturity results in organized and complex

functional communities with numerous microorganisms embedded in a self-produced matrix composed of extracellular polymeric substances (EPS).<sup>3–5</sup> This heterogeneous structure provides several advantages to sessile microorganisms, compared to those living as planktonic or free-floating cells, such as the ability to evade both antibiotic agents and the human immune responses.<sup>4–6</sup> Additionally, focal areas of biofilm can detach into surrounding tissues and in the circulatory system giving rise to septicemia, or spread to another location where

\*These authors contributed equally to this work.

**Correspondence to:** J. Barros; i3S – Instituto de Investigação e Inovação em Saúde, Rua Alfredo Allen, 208, 4200-135 Porto, Portugal; e-mail: joana.barros@ineb.up.pt

Contract grant sponsor: Programa Operacional Factores de Competitividade (COMPETE)

Contract grant sponsor: NaNOBiofilm project, Fundação para a Ciência e a Tecnologia (FCT); contract grant number: PTDC/SAU-BMA/111233/2009

Contract grant sponsor: Joana Barros' PhD grant, Fundação para a Ciência e Tecnologia (FCT); contract grant number: SFRH/BD/102148/2014

Contract grant sponsor: Liliana Grenho's PhD grant, Fundação para a Ciência e Tecnologia (FCT); contract grant number: SFRH/BD/72866/2010

new biofilms can be formed.<sup>7</sup> Although the incidence of implant-related infections has been drastically reduced due to the modern medical facilities and the aseptic measures, they still pose a serious problem as the number of implanted devices continues to rise, followed by high morbidity and substantial medical and social costs.<sup>1,8,9</sup>

The majority of implant-associated infections are caused by staphylococci, especially coagulase-negative staphylococci (e.g., *Staphylococcus epidermidis*) and *Staphylococcus aureus*, followed by streptococci, enterococci, Gram-negative bacilli (e.g., *Escherichia coli* and *Pseudomonas aeruginosa*), and yeasts.<sup>8,10–12</sup> Polymicrobial infections are reported in about 10–11% of the cases, depending on the quality of the diagnostic procedure and preceding antimicrobial therapy.<sup>2,11</sup> In contrast to most other infections, implant-associated infections are highly resistant to antibiotherapy and they tend to persist until the device is surgically removed.<sup>2</sup> Owing to this recognized difficulty in eradicating antibiotic-resistant biofilms, the prevention of infection following device implantation continues to be the focus of intense research in the biomedical field. In orthopedic surgery, embedding or loading antimicrobial substances into nanophased ceramics is a promising new approach.<sup>13</sup> The local delivery of bioactive agents has several advantages as it maximizes their effect where they are required, for prolonged periods of time, to produce the desired outcomes, with reduced potential systemic toxicity and cost efficiency.<sup>14</sup> Among the biomaterials used for bone-related applications, nanohydroxyapatite (nanoHA) possesses exceptional bioactive and osteoconductive properties due to its biomimetic chemistry and morphology when compared to mineral bone phase. NanoHA bonds to bone and enhances bone tissue formation justifying its use as a coating material or as a bone substitute.<sup>15–17</sup> In this context, and to avoid the use of common antibiotics and minimize the antibiotic-resistant rate, different approaches may be designed with different organic and inorganic antimicrobial agents. In this work, chlorhexidine digluconate (CHX), an organic agent, was compared to zinc oxide (ZnO) nanoparticles, an inorganic metal oxide, when they were added to nanoHA substrate. The materials' antibiofilm properties against single- and dual-species biofilms of *S. aureus* and *E. coli* were assessed and compared.

## MATERIALS AND METHODS

### Preparation of nanoHA-based materials

NanoHA disc samples, 5 mm diameter and 1 mm height, were prepared as previously described.<sup>18</sup> Briefly, nanoHA powder (nanoXIM-HAp202; Fluidinova S.A.) was pressed as cylindrical samples in an uniaxial press and thereafter sintered at 830°C with a 15 min plateau and applying a heating rate of 20°C min<sup>-1</sup>. The sintering cycle was completed with a natural cooling process inside the furnace. The discs were sterilized by dry heat (180°C, 2 h). The adsorption of CHX onto nanoHA discs (nanoHA-CHX) was performed as described elsewhere.<sup>19</sup> Shortly, nanoHA discs were aseptically incubated with 5 mL of 0.05 mg mL<sup>-1</sup> CHX (Sigma-Aldrich) for 24 h at 37°C and 60 rpm. NanoHA discs incubated with sterile deionized water were used as control. Regarding nanoHA-ZnO composite discs,

they were prepared as formerly described.<sup>20</sup> Briefly, the composite powder was prepared by mixing as-received ZnO nanoparticles (<50 nm particle size, Sigma-Aldrich) with nanoHA powder at weight percentages (wt %) of 2, and subsequently pressed as cylindrical samples. The discs were sintered and sterilized as aforementioned.

### Microorganisms and culture conditions

The reference strains *S. aureus* ATCC 25923 and *E. coli* ATCC 25922 were used. Prior to each experiment, bacteria were cultured in Tryptic Soy Broth (TSB, Merck Millipore) for 24 h at 37°C and 150 rpm. Standardized bacterial suspensions for single- and dual-biofilms formation were then prepared in TSB in the required concentrations, detailed below.

### Biofilm formation on nanoHA-based materials

For single-species biofilms, 200 µL of *S. aureus* or *E. coli* cultures at  $1.25 \times 10^8$  cells mL<sup>-1</sup> were used, while for dual-species biofilms, 100 µL cultures of each bacteria at an initial concentration of  $2.5 \times 10^8$  cells mL<sup>-1</sup> were used. Bacterial suspensions were transferred into wells of a 96-well treated culture plate (Falcon) containing the nanoHA-based materials namely nanoHA-CHX, nanoHA-ZnO, and pure nanoHA, as control. Plates were incubated at 37°C and 150 rpm during 24 h to allow biofilm formation. After incubation, the medium was removed and nanoHA-based materials were rinsed twice with sterile saline (0.9% NaCl, J.T.Baker) to remove nonadherent and weakly adherent bacteria. Biofilm growth was quantified by the enumeration of colony-forming units (CFUs), and qualitatively analyzed by confocal microscopy, using both Live/Dead staining and *in situ* hybridization, and by scanning electron microscopy (SEM), as detailed below.

### Cultivable cell number

Prewashed discs were aseptically transferred to tubes containing 5 mL sterile saline and sonicated in an ultrasonic bath (Transsonic 420, 70 W, 35 kHz, ELMA) for 10 min to dislodge sessile bacteria. The resulting suspensions were serially diluted, and inoculated onto agar plates, specifically Plate Count Agar (PCA, Liofilchem) to quantify the total number of cultivable cells; Manitol Salt Agar (MSA, Liofilchem) and MacConkey Agar (MCA, Liofilchem) to isolate and selectively quantify *S. aureus* and *E. coli*, respectively. After 24 h incubation at 37°C, the CFUs were counted and expressed as CFU cm<sup>-2</sup>.

### Live/Dead biofilm staining

Prewashed discs of each nanoHA-based material were stained using the Live/Dead<sup>®</sup> BacLight viability kit (Invitrogen), for 10 min in the dark at room temperature. The biofilm structure was imaged using Spectral Confocal Microscopy (Leica TCS SP5), wherein the living biofilm bacteria appeared as green in color (due to SYTO 9), while bacteria with compromised membranes were red (due to propidium iodide, PI).

### Fluorescent *in situ* hybridization (FISH)

FISH was used to visualize and discriminate detached bacteria species from nanoHA-based materials, after samples sonication, as described above. Specific DNA probes were used.

The probe Sau 16S69 (5'-Alexa 546-GAAGCAAGCTTCTCGTC CG-3') detects specifically *S. aureus* as previously described by Poppert et al. (2010) and Lawson et al. (2011).<sup>21,22</sup> *E. coli*-specific probe Col23S1502 (5'-Alexa 488-CACGCCTC AGCCTTGATT-3') was designed based on Azevedo et al.'s (2015) study.<sup>23</sup> Both probes were purchased from Thermo Fisher Scientific. Single-species biofilms were used as control.

The hybridization process was based on procedures described by Fontenete et al. (2015),<sup>24</sup> with few modifications. After detachment, bacterial cells were centrifuged at 14,000 rpm for 15 min. After supernatant discharge, the bacteria were resuspended in 400  $\mu\text{L}$  of 4% (v/v) paraformaldehyde (Sigma-Aldrich) for 1 h, followed by centrifugation at 14,000 rpm for 5 min. The fixed cells were resuspended in 500  $\mu\text{L}$  of 70% ethanol and incubated at  $-20^{\circ}\text{C}$  for at least 30 min. Permeabilization was conducted by adding 30  $\mu\text{L}$  of lysozyme (2 mg  $\text{mL}^{-1}$ ; Sigma-Aldrich) in Tris/HCl (pH 8) and incubated at  $37^{\circ}\text{C}$  for 1 h. Afterward, 100  $\mu\text{L}$  of fixed cells were resuspended in 100  $\mu\text{L}$  of hybridization solution containing 30% (v/v) formamide (Sigma-Aldrich), 0.9 mol  $\text{mL}^{-1}$  NaCl, 50 mM Tris-HCl, 0.01% (w/v) SDS, and 25 nM of each probe and incubated at  $48^{\circ}\text{C}$  for 3 h. For each experiment, a negative control was performed simultaneously following all the steps but without the addition of the probe to the hybridization solution. After hybridization, the samples were centrifuged at 14,000 rpm for 5 min, resuspended in 500  $\mu\text{L}$  of washing solution (0.64 mL  $\text{L}^{-1}$  NaCl, 5 mM Tris-HCl, 0.01% (w/v) SDS) and incubated at  $48^{\circ}\text{C}$  for 20 min. The cells were lastly centrifuged at 14,000 rpm for 5 min and resuspended in 500  $\mu\text{L}$  of saline. The bacterial suspensions were filtered in a black Nucleopore polycarbonate membrane ( $\varnothing$  25 mm) with a pore size of 0.2  $\mu\text{m}$  (Whatman) and observed by Spectral Confocal Microscopy (Leica TCS SP5).

### Scanning electron microscopy (SEM)

SEM analyses were held to directly observe sessile bacteria on nanoHA-based materials surface, for either single- or dual-species biofilms. Prewashed samples were initially fixed for 30 min with 3% glutaraldehyde (Sigma-Aldrich) and then slowly dehydrated in a gradient ethanol series for 10 min each. Samples were subsequently dried in a gradient series of hexamethyldisilazane (HMDS, Sigma-Aldrich) solutions for 10 min each. NanoHA samples were fixed on sample holders with double-sided carbon tape and sputter-coated (SPI-Module) with a conductive gold-palladium film. Biofilms were imaged using a FEI Quanta 400 FEG/ESEM microscope (FEI, USA) operated at 15 kV.

### Statistical analysis

All experiments were performed in triplicate and repeated in three independent assays. Statistical analysis was performed using SPSS software (IBM<sup>®</sup> version 20.0). The number of adherent bacteria on nanoHA-modified materials was compared to control, pure nanoHA, using one-way analysis of variance (ANOVA) and Tukey HSD multiple comparison *post hoc* test. Comparative analyses between nanoHA-modified materials and between bacteria were also performed using independent-samples *t* test. Differences were considered statistically significant at a *p* value of  $<0.05$ .

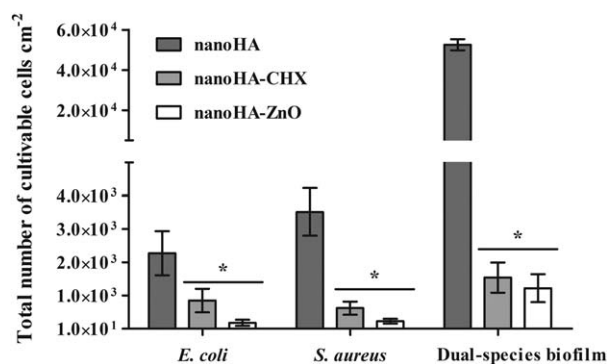


**FIGURE 1.** Sessile population for single- and dual-species biofilms experiments, on nanoHA-based materials, after 24 h incubation (\* $p < 0.05$ , significant differences compared to pure nanoHA).

## RESULTS

### Antibiofilm effect of nanoHA-based materials

**Cultivable cell number.** After 24 h incubation, the total number of cultivable sessile cells on nanoHA-based materials for either single- or dual-species biofilms was quantified (Fig. 1). Regarding single-species biofilms assays, *S. aureus* showed higher ability to adhere on pure nanoHA materials ( $3.5 \times 10^3$  CFUs  $\text{cm}^{-2}$ ) than *E. coli* ( $2.3 \times 10^3$  CFUs  $\text{cm}^{-2}$ ). A strong and significant decrease in the number of adherent bacterial cells was observed for both nanoHA-modified materials, particularly for *S. aureus* biofilm, compared with pure nanoHA. Wherein, a reduction over 80% was observed for nanoHA-CHX and over 90% for nanoHA-ZnO. Regarding *E. coli* biofilm, it was also observed that nanoHA-modified materials showed a significant reduction, which was higher than 60% and 90% for nanoHA-CHX and nanoHA-ZnO, respectively. However, between nanoHA-modified materials and both bacteria did not observe significant differences. Concerning dual-species biofilms, the number of sessile cells increased in one log for all nanoHA-based materials, as compared to single-species biofilms (Fig. 1). Still, nanoHA-modified materials exhibited a strong and significant decrease in the number of adherent cells, around 97%, comparatively to pure nanoHA.

To further discriminate and quantify *E. coli* and *S. aureus* within dual-species biofilm, selective growth media were used (Fig. 2). The number of sessile *E. coli* on materials surface was statistically higher than that obtained for *S. aureus*, regardless of the materials used.

### Live/Dead biofilm staining

Bacterial viability was also evaluated through direct observation of sessile cells on nanoHA-based materials surface after Live/Dead staining (Fig. 3.1). The recorded observations were rather similar to those obtained by cultivable cell techniques. For instance, on pure nanoHA, most of the cells were alive for either *S. aureus* or *E. coli* biofilms, while on nanoHA-modified materials, the amount of living bacterial cells was considerably lower; that is, the modifications were effective in preventing biofilm formation (Fig. 3.1). The recorded observations also confirmed the higher ability of *S. aureus* to form biofilm on nanoHA, comparatively to

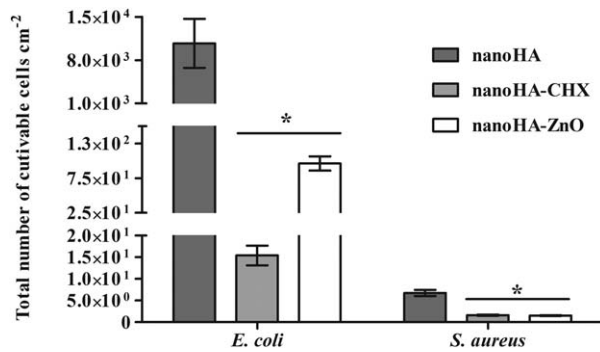


**FIGURE 2.** Bacterial discrimination within dual-species biofilms, for each nanoHA-based material, after 24 h incubation (\* $p < 0.05$ , significant differences compared to pure nanoHA).

*E. coli*. Concerning dual-species biofilms, all nanoHA-based materials exhibited the spread of living biofilms, which was higher than those in single-species biofilms. Still, nanoHA-modified materials showed to be efficient against dual-species biofilm, where the amount of bacterial cells was significantly lower than that on pure nanoHA materials (Fig. 3.1).

### FISH

FISH methodology was used to qualitatively discriminate detached bacterial cells from single- and dual-species biofilms formed on nanoHA-based materials. For that purpose, two probes that specifically detected regions of *S. aureus* 16S rRNA and *E. coli* 23S rRNA were used. The hybridization conditions were optimized for the target microorganisms, and

probes specificity was confirmed on pure cultures. Both probes provided a strong fluorescent signal at 48°C and no cross-hybridization was observed between probes (data not shown).

The number of dislodged cells from pure nanoHA materials was higher for *S. aureus* than for *E. coli* (Fig. 3.2). Regarding dual-species biofilm on pure nanoHA materials, the confocal images showed that most of the detached bacterial cells emitted green fluorescence, that is, *E. coli* was the predominant species detached from dual-species biofilm structure (Fig. 3.2), which is in accordance with CFU data. Additionally, some aggregates appeared as yellow/orange, due to the overlapping of green and red fluorescence that indicates the aggregation of *E. coli* and *S. aureus* (Fig. 3.2). For single- and dual-species biofilms on nanoHA-modified materials, no fluorescence signal was detected.

### SEM

SEM observations are overall consistent with the results previously described. For instance, in single-species biofilm, either *S. aureus* or *E. coli* cells were spread throughout the surface of pure nanoHA (Fig. 3.3). In contrast, on nanoHA-modified materials, low cell density was observed, regardless the antimicrobial agent used, for either single- or dual-species biofilms (data not shown). SEM provided further relevant data regarding sessile population arrangement on pure nanoHA surfaces for dual-species biofilm assays, namely a stratified growth, wherein *E. coli* was directly laid up on the nanoHA surfaces and *S. aureus* appeared on the top layer (Fig. 3.3).

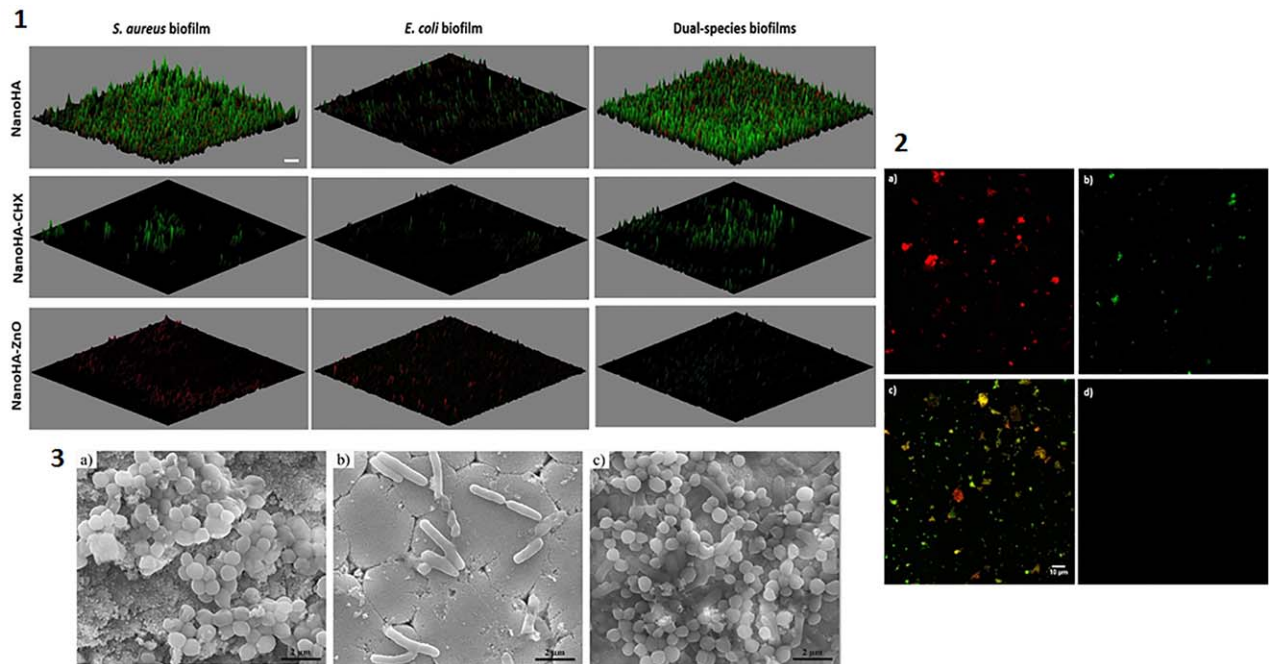


**FIGURE 3.** Single- and dual-species biofilms on nanoHA-based materials obtained by confocal microscopy after Live/Dead staining. Scale bar 10  $\mu\text{m}$  (1); and after FISH performed in detached bacterial cells: (2a) *S. aureus* biofilm (red fluorescence); (2b) *E. coli* biofilm (green fluorescence); (2c) dual-species biofilm; (d) negative control without probes. Scale bar 10  $\mu\text{m}$ . SEM images of single-species biofilms of (3a) *S. aureus* and (3b) *E. coli* and (3c) dual-species biofilms on pure nanoHA substrates. Scale bar 2  $\mu\text{m}$ .

## DISCUSSION

Currently, efforts have been put on the development of novel materials to produce medical devices able to provide an adequate interface with living tissues and display potential for drug delivery to fight infections. Among them, nanoHA biomaterials are widely used in orthopedic and dental applications, given its unique surface properties as high surface area, porosity, and densification, which improve its mechanical properties under load, solubility *in vivo*, and the capacity to penetrate cell membranes. Its nanoscale topography has also a positive effect on osteoblastic proliferation and differentiation, resulting in improved biocompatibility and osteointegration. Additionally, nanoHA has the capacity to be a vehicle for the transport of biochemical factors or drugs. Some authors have addressed the capacity of blending nanoHA with antimicrobial agents (e.g., amoxicillin, erythromycin, minocycline, cobalt) or materials (e.g., chitosan), either by loading them on the biomaterial surface or by mixing with the bulk material.<sup>15,25-27</sup> These strategies possess significant advantages over systemic drug delivery therapy, namely, the applicability of lower doses, long-term effect, and reduced systemic toxicity.<sup>14</sup>

In this work, both approaches were tested with two different antimicrobial agents: CHX was adsorbed on nanoHA surfaces, while ZnO nanoparticles were integrated into nanoHA substrates. Antibiofilm properties of both approaches against single- and dual-species biofilms of *S. aureus* and *E. coli* were assessed. These bacteria are the most common etiological agents of medical devices-related infections, which can produce single or mixed species-biofilms on implant surfaces.

NanoHA-modified materials revealed to have a strong antibiofilm effect against single-species biofilm of *S. aureus* and *E. coli*, which is in accordance with previous studies.<sup>19,20,28</sup> Both antimicrobial agents (CHX and ZnO nanoparticles) have a large broad spectrum of antimicrobial activity comprising Gram-positive and Gram-negative bacteria as well as yeasts. Through different mechanisms of action, both antimicrobial agents interfere with cellular metabolic processes and osmotic control that, subsequently, lead to irreversible damage to the microorganisms.<sup>29-31</sup> In this work, it was also observed that *S. aureus* was more sensitive to nanoHA-modified materials than *E. coli*, as obtained by other authors.<sup>19,20</sup>

Concerning dual-species biofilms, an increase in biofilm density was observed for all materials assessed, still nanoHA-modified materials showed strong antibiofilm activity. These results indicate that both approaches can be applied in the treatment of single- and dual-species biofilms. Additionally, dual-species biofilms experiments showed a competition between bacteria, where *E. coli* was the outcompeting species. *E. coli* showed higher proliferative capacity, whereas *S. aureus* growth was inhibited by *E. coli* presence. Competition between bacterial species has also been reported by other authors. Stoodly et al. (2012) showed that in the case of a mixed *S. aureus* and *Enterococcus faecalis* biofilm, the relative abundances of the two bacteria changed dramatically over time, proving that biofilm composition and physiology are by no means static.<sup>32</sup> In another study, uropathogenic and commensal *E. coli* strains were shown to release a soluble

polysaccharide that modulates bacterial adhesion and prevents biofilm formation by other Gram-negative or Gram-positive bacteria.<sup>33</sup> A step ahead, Rendueles et al. (2011) showed that *E. coli* Ec300 biofilms produced the Ec300 polysaccharide (Ec300p) that provided rapid exclusion of *S. aureus* from mixed *E. coli* and *S. aureus* biofilms. This study clearly shows that the release of antiadhesion polysaccharides, as Ec300p, confers a competitive advantage with respect to the producing strain, at the initial colonization stage, and it could significantly contribute to colonization resistance against strong colonizers.<sup>34</sup> This colonization resistance could also involve other mechanisms. Surface motility mediated by motility organelles represents indeed another important parameter that not only shapes the spatial distribution within a mixed biofilm but can also enable one species to outcompete the others. Experiments conducted by Wood et al. (2006) revealed that the best *E. coli* biofilm-former strains displayed the highest motility, linking the phenomena of motility and biofilm development.<sup>35</sup> The flagella that are used for swimming motility can also act as initial adhesion points. This rapid and efficient occupancy of all available adhesion sites, referred to as “surface blanketing,” can be one of the simplest strategies to avoid initial colonization of competing strains.<sup>36</sup> Similar evidences were observed in this study. The visualization of bacterial communities from dual-species biofilms through SEM revealed that bacteria were arranged in layers, where on nanoHA surfaces, *E. coli* was the most prevalent species directly attached to the material surface while *S. aureus* appeared at the top layer of the biofilm. Moreover, FISH technique confirmed the overlapping of bacteria, proven by the fluorescence overlapping. Such spatial arrangement could be related with *E. coli* motility, which is playing a crucial role to first reach the surface.

In fact, different mechanisms may be involved in the observed interaction between bacterial species within polymicrobial biofilms and such interactions can dictate the selection and colonization of the best-adapted microorganisms.<sup>36-38</sup> As a consequence, the medical community is increasingly recognizing the significance of polymicrobial interactions associated with human health and diseases.<sup>39</sup> Polymicrobial biofilm infections have already been implicated in oral cavity diseases, otitis media, diabetic foot wound infections, cystic fibrosis, and infected implants.<sup>40-42</sup> In such cases, the composition of microbial populations predicts disease severity and treatment outcome.<sup>43</sup> Thereby, studies involving different bacterial species on biofilm formation are required to better understand polymicrobial biofilm infections and, thus to choose the best therapeutic approaches.

## CONCLUSION

Biofilms play an important role in nature, in industry, and in medical ecosystems. They are harmful by inducing resilient infections. As with any infection, prevention is the preferred control option, but when there is a risk of biofilm formation, prevention becomes even more critical. In this work, the antibiofilm properties of nanoHA-CHX and nanoHA-ZnO materials against single- and dual-species biofilms of *S. aureus* and

*E. coli* were assessed. The preventive strategies explored in this work revealed to be successful to minimize single- and dual-species biofilms. Interesting competitions for two-species community were observed, where *E. coli* was the out-competing species. Either adsorbed CHX or integrated ZnO nanoparticles have several interesting features such as low doses application, long-term effect, and reduced systemic toxicity. These strategies have the additional advantage of not inducing microbial resistance, often associated to the use of antibiotic-loaded biomaterials.

## ACKNOWLEDGMENTS

The authors are thankful to Fluidinova S.A., Portugal, for the provision of NanoXIM.

## REFERENCES

- McConoughey SJ, Howlin R, Granger JF, Manring MM, Calhoun JH, Shirliff M, Kathju S, Stoodley P. Biofilms in periprosthetic orthopedic infections. *Future Microbiol* 2014;9:987–1007.
- Zimmerli W, Moser C. Pathogenesis and treatment concepts of orthopaedic biofilm infections. *FEMS Immunol Med Microbiol* 2012;65:158–168.
- Hoiby N, Ciofu O, Johansen HK, Song ZJ, Moser C, Jensen PO, Molin S, Givskov M, Tolker-Nielsen T, Bjarnsholt T. The clinical impact of bacterial biofilms. *Int J Oral Sci* 2011;3:55–65.
- Burmolle M, Webb JS, Rao D, Hansen LH, Sorensen SJ, Kjelleberg S. Enhanced biofilm formation and increased resistance to antimicrobial agents and bacterial invasion are caused by synergistic interactions in multispecies biofilms. *Appl Environ Microbiol* 2006;72:3916–3923.
- Costerton JW, Stewart PS, Greenberg EP. Bacterial biofilms: a common cause of persistent infections. *Science* 1999;284:1318–1322.
- Hoiby N, Bjarnsholt T, Givskov M, Molin S, Ciofu O. Antibiotic resistance of bacterial biofilms. *Int J Antimicrob Agents* 2010;35:322–332.
- Hall-Stoodley L, Stoodley P. Evolving concepts in biofilm infections. *Cell Microbiol* 2009;11:1034–1043.
- Fernandes A, Dias M. The microbiological profiles of infected prosthetic implants with an emphasis on the organisms which form biofilms. *J Clin Diagn Res* 2013;7:219–223.
- Ribeiro M, Monteiro FJ, Ferraz MP. Infection of orthopedic implants with emphasis on bacterial adhesion process and techniques used in studying bacterial-material interactions. *Biomater* 2012;2:176–194.
- Cauda R. Candidaemia in patients with an inserted medical device. *Drugs* 2009;69:33–38.
- Arciola CR, An YH, Campoccia D, Donati ME, Montanaro L. Etiology of implant orthopedic infections: a survey on 1027 clinical isolates. *Int J Artif Organs* 2005;28:1091–1100.
- Montanaro L, Speziale P, Campoccia D, Ravaoli S, Cangini I, Pietrocola G, Giannini S, Arciola CR. Scenery of *Staphylococcus* implant infections in orthopedics. *Future Microbiol* 2011;6:1329–1349.
- Simchi A, Tamjid E, Pishbin F, Boccaccini AR. Recent progress in inorganic and composite coatings with bactericidal capability for orthopaedic applications. *Nanomedicine* 2011;7:22–39.
- Wu P, Grainger DW. Drug/device combinations for local drug therapies and infection prophylaxis. *Biomaterials* 2006;27:2450–2467.
- Ferraz MP, Monteiro FJ, Manuel CM. Hydroxyapatite nanoparticles: a review of preparation methodologies. *J Appl Biomater Biomech* 2004;2:74–80.
- Roveri N, Iafisco M. Evolving application of biomimetic nanostructured hydroxyapatite. *Nanotechnol Sci Appl* 2010;3:107–125.
- Zhou H, Lee J. Nanoscale hydroxyapatite particles for bone tissue engineering. *Acta Biomater* 2011;7:2769–2781.
- Barros J, Grenho L, Manuel CM, Ferreira C, Melo L, Nunes OC, Monteiro FJ, Ferraz MP. Influence of nanohydroxyapatite surface properties on *Staphylococcus epidermidis* biofilm formation. *J Biomater Appl* 2014;28:1325–1335.
- Barros J, Grenho L, Fernandes MH, Manuel CM, Melo LF, Nunes OC, Monteiro FJ, Ferraz MP. Anti-sessile bacterial and cytocompatibility properties of CHX-loaded nanohydroxyapatite. *Colloids Surf B* 2015;130:305–314.
- Grenho L, Monteiro FJ, Pia Ferraz M. *In vitro* analysis of the antibacterial effect of nanohydroxyapatite-ZnO composites. *J Biomed Mater Res A* 2014;102:3726–3733.
- Poppert S, Riecker M, Wellinghausen N, Frickmann H, Essig A. Accelerated identification of *Staphylococcus aureus* from blood cultures by a modified fluorescence *in situ* hybridization procedure. *J Med Microbiol* 2010;59:65–68.
- Lawson TS, Connally RE, Vemulapad S, Piper JA. Optimization of a two-step permeabilization fluorescence *in situ* hybridization (FISH) assay for the detection of *Staphylococcus aureus*. *J Clin Lab Anal* 2011;25:359–365.
- Azevedo AS, Almeida C, Pereira B, Madureira P, Wengel J, Azevedo NF. Detection and discrimination of biofilm populations using locked nucleic acid/2'-O-methyl-RNA fluorescence *in situ* hybridization (LNA/2'OMe-FISH). *Biochem Eng J* 2015;104:64–73.
- Fontenete S, Barros J, Madureira P, Figueiredo C, Wengel J, Azevedo NF. Mismatch discrimination in fluorescent *in situ* hybridization using different types of nucleic acids. *Appl Microbiol Biotechnol* 2015;99:3961–3969.
- Ferraz MP, Mateus AY, Sousa JC, Monteiro FJ. Nanohydroxyapatite microspheres as delivery system for antibiotics: Release kinetics, antimicrobial activity, and interaction with osteoblasts. *J Biomed Mater Res A* 2007;81A:994–1004.
- Zamanian A, Moztafzadeh F, Kordestani S, Hesarak S, Tahriri M. Novel calcium hydroxide/nanohydroxyapatite composites for dental applications: *in vitro* study. *Adv Appl Ceram* 2010;109:440–444.
- Shi P, Zuo Y, Li X, Zou Q, Liu H, Zhang L, Li Y, Morsi YS. Gentamicin-impregnated chitosan/nanohydroxyapatite/ethyl cellulose microspheres granules for chronic osteomyelitis therapy. *J Biomed Mater Res A* 2010;93:1020–1031.
- Grenho L, Salgado CL, Fernandes MH, Monteiro FJ, Ferraz MP. Antibacterial activity and biocompatibility of three-dimensional nanostructured porous granules of hydroxyapatite and zinc oxide nanoparticles—an *in vitro* and *in vivo* study. *Nanotechnology* 2015;26:315101.
- Barbour ME, O'Sullivan DJ, Jagger DC. Chlorhexidine adsorption to anatase and rutile titanium dioxide. *Colloids Surf A Physicochem Eng Asp* 2007;307:116–120.
- Applerot G, Lipovsky A, Dror R, Perkas N, Nitzan Y, Lubart R, Gedanken A. Enhanced antibacterial activity of nanocrystalline ZnO due to increased ROS-mediated cell injury. *Adv Funct Mater* 2009;19:842–852.
- Stoimenov PK, Klinger RL, Marchin GL, Klabunde KJ. Metal oxide nanoparticles as bactericidal agents. *Langmuir* 2002;18:6679–6686.
- Stoodley P, Sidhu S, Nistico L, Mather M, Boucek A, Hall-Stoodley L, Kathju S. Kinetics and morphology of polymicrobial biofilm formation on polypropylene mesh. *FEMS Immunol Med Microbiol* 2012;65:283–290.
- Valle J, Da Re S, Henry N, Fontaine T, Balestrino D, Latour-Lambert P, Ghigo JM. Broad-spectrum biofilm inhibition by a secreted bacterial polysaccharide. *Proc Natl Acad Sci USA* 2006;103:12558–12563.
- Rendueles O, Travier L, Latour-Lambert P, Fontaine T, Magnus J, Denamur E, Ghigo JM. Screening of *Escherichia coli* species biodiversity reveals new biofilm-associated antiadhesion polysaccharides. *MBio* 2011;2:e00043-11.
- Wood TK, Gonzalez Barrios AF, Herzberg M, Lee J. Motility influences biofilm architecture in *Escherichia coli*. *Appl Microbiol Biotechnol* 2006;72:361–367.
- Rendueles O, Ghigo JM. Multi-species biofilms: how to avoid unfriendly neighbors. *FEMS Microbiol Rev* 2012;36:972–989.
- Elias S, Banin E. Multi-species biofilms: living with friendly neighbors. *FEMS Microbiol Rev* 2012;36:990–1004.
- Yang L, Liu Y, Wu H, Hoiby N, Molin S, Song ZJ. Current understanding of multi-species biofilms. *Int J Oral Sci* 2011;3:74–81.

39. Brogden KA, Guthmiller JM, Taylor CE. Human polymicrobial infections. *Lancet* 2005;365:253–255.
40. Armbruster CE, Hong W, Pang B, Weimer KED, Juneau RA, Turner J, Swords WE. Indirect pathogenicity of *Haemophilus influenzae* and *Moraxella catarrhalis* in polymicrobial otitis media occurs via interspecies quorum signaling. *mBio* 2010;1:1–10.
41. Thornton RB, Rigby PJ, Wiertsema SP, Filion P, Langlands J, Coates HL, Vijayasekaran S, Keil AD, Richmond PC. Multi-species bacterial biofilm and intracellular infection in otitis media. *BMC Pediatrics* 2011;11:
42. Kathju S, Nistico L, Melton-Kreft R, Lasko LA, Stoodley P. Direct demonstration of bacterial biofilms on prosthetic mesh after ventral herniorrhaphy. *Surg Infect* 2015;16:45–53.
43. Peters BM, Jabra-Rizk MA, O'May GA, Costerton JW, Shirtliff ME. Polymicrobial interactions: impact on pathogenesis and human disease. *Clin Microbiol Rev* 2012;25:193–213.